BBA - Gene Regulatory Mechanisms 1867 (2024) 195048

Contents lists available at ScienceDirect

BBA - Gene Regulatory Mechanisms

journal homepage: www.elsevier.com/locate/bbagrm

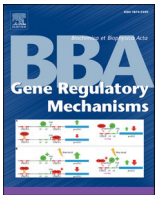

# H3K56 acetylation affects *Candida albicans* morphology and secreted soluble factors interacting with the host

Marisa Conte [a,b,1], Daniela Eletto [a,1], Martina Pannetta [a,b], Roberta Esposito [a], Maria Chiara Monti [a,c], Elva Morretta [a], Peter Tessarz [d,e,f,2], Silvana Morello [a], Alessandra Tosco [a,*], Amalia Porta [a,*]

[a] Department of Pharmacy, University of Salerno, Fisciano (SA), Italy
[b] Ph.D. Program in Drug Discovery and Development, University of Salerno, Fisciano (SA), Italy
[c] Department of Pharmacy, University of Naples "Federico II", Italy
[d] Max Planck Research Group "Chromatin and Ageing", Max Planck Institute for Biology of Ageing, University of Cologne, Germany
[e] Cologne Excellence Cluster on Stress Responses in ageing-associated Diseases (CECAD), University of Cologne, Germany
[f] Dept. Of Human Biology, Radboud Institute for Molecular Life Sciences, Faculty of Science, Radboud University, Nijmegen, the Netherlands

ARTICLE INFO

*Keywords:*
*Candida albicans*
Macrophage response
Farnesol
H3K56 acetylation
ChIP-seq
RNA-seq

ABSTRACT

In recent years, epigenetics has been revealed as a mechanism able to modulate the expression of virulence traits in diverse pathogens, including *Candida albicans*. Indeed, epigenetic regulation can sense environmental changes, leading to the rapid and reversible modulation of gene expression with consequent adaptation to novel environments. How epigenetic changes can impact expression and signalling output, including events associated with mechanisms of morphological transition and virulence, is still poorly studied. Here, using nicotinamide as a sirtuin inhibitor, we explored how the accumulation of the H3K56 acetylation, the most prominent histone acetylation in *C. albicans*, might affect its interaction with the host. Our experiments demonstrate that H3K56 acetylation profoundly affects the production and/or secretion of soluble factors compromising actin remodelling and cytokine production. ChIP- and RNA-seq analyses highlighted a direct impact of H3K56 acetylation on genes related to phenotypic switching, biofilm formation and cell aggregation. Direct and indirect regulation also involves genes related to cell wall protein biosynthesis, β-glucan and mannan exposure, and hydrolytic secreted enzymes, supporting the hypothesis that the fluctuations of H3K56 acetylation in *C. albicans* might impair the macrophage response to the yeast and thus promote the host-immune escaping.

## 1. Introduction

*Candida albicans* is a well-adapted commensal fungus that colonises mucosal regions like the mouth, gut, and vagina. However, in immunocompromised hosts or following prolonged antibacterial treatments, it might act as an opportunistic pathogen, causing invasive diseases up to life-threatening systemic infections [1]. Among the various mechanisms developed by the fungus to switch from commensal to deadly pathogen, there are: i) reversible morphological transition between yeast and filamentous forms, ii) white-opaque phenotypic switch and iii) biofilm formation [2]. Each of these strategies is potentially pathogenic since they favour *C. albicans* adherence, tissue invasion, and the formation of resilient biofilm communities on medical devices and host surfaces.

Central to the interplay between *C. albicans* and the host immune system are innate immune phagocytes, particularly macrophages (MΦs) [3]. These cells play a crucial role in recognizing and eliminating fungal pathogens through pattern recognition receptors (PRRs) that detect pathogen-associated molecular patterns (PAMPs) present on the surface of *C. albicans*, mainly cell wall carbohydrates as mannans (in

*Abbreviations:* macrophages, MΦs; Pattern recognition receptors, PRRs; pathogen-associated molecular patterns, PAMPs; quorum sensing molecules, QSMs; farnesol, FOH; nicotinamide, NAM.

* Corresponding authors.
*E-mail addresses:* tosco@unisa.it (A. Tosco), aporta@unisa.it (A. Porta).

[1] These authors equally contributed.
[2] Present address.

https://doi.org/10.1016/j.bbagrm.2024.195048
Received 8 March 2024; Received in revised form 17 May 2024; Accepted 10 June 2024
Available online 15 June 2024

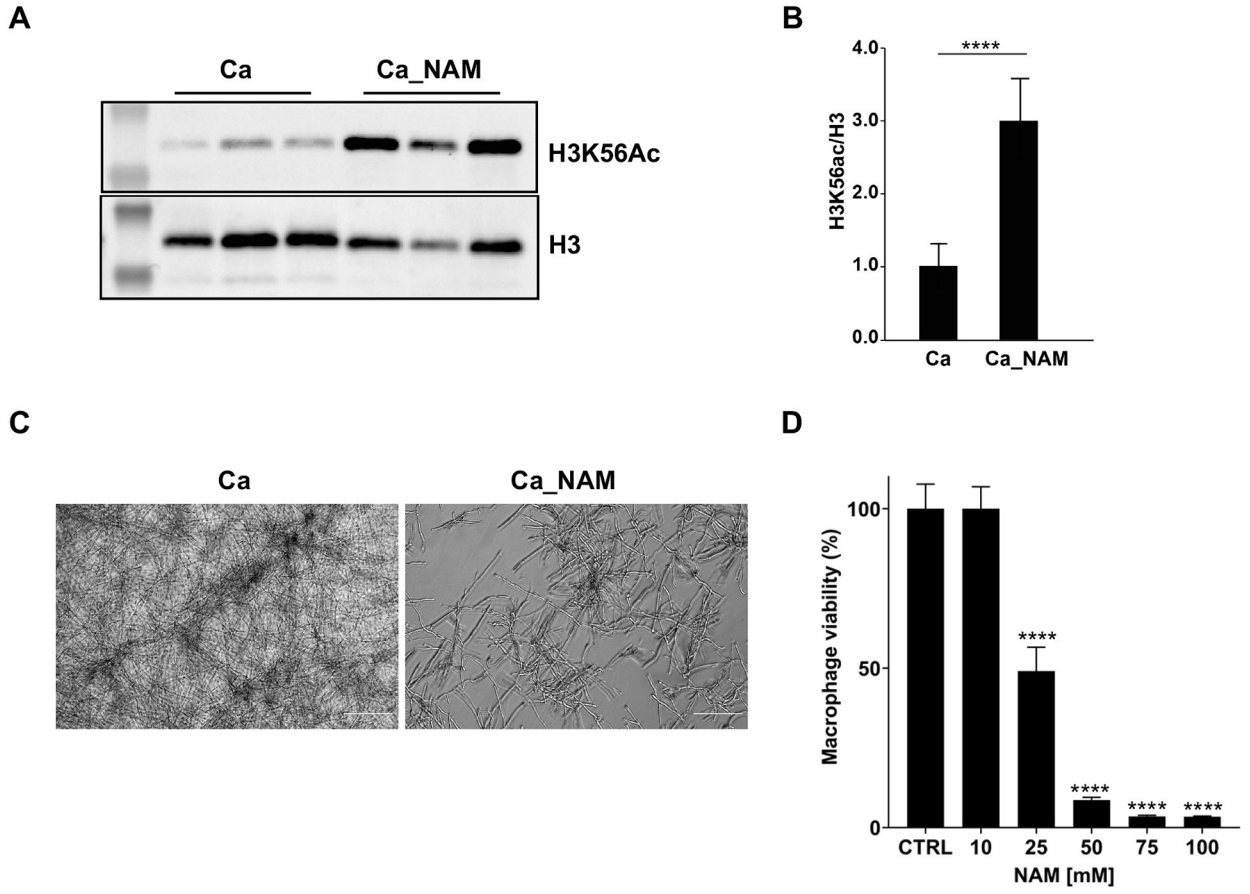


**Fig. 1.** NAM treatment reduces hyphae formation. **(A)** *C. albicans* (Ca) was grown with or without 10 mM NAM in hyphae-promoting conditions, and the H3K56ac signal was detected by Western Blot in three independent experiments. Total H3 served as loading control. **(B)** Densitometric analysis of H3K56ac normalised to H3 from the Western Blot in (A). Values are the mean ± standard deviation of three independent experiments ****$p < 0.0001$ (*t*-test). **(C)** Representative pictures of *C. albicans* cells incubated overnight without (Ca) or with 10 mM NAM (Ca_NAM) in RPMI at 37 °C. Scale bar: 100 μm. **(D)** Viability of J774A.1 cells by MTT assay following the treatment with different concentrations of NAM for 24 h. Values are the mean ± s.d. of four replicates. **** $p < 0.0001$ (one-way ANOVA with Dunnet's test).

glycosylated proteins), β-glucan, and chitin [4,5]. However, *C. albicans* has developed sophisticated mechanisms to evade macrophage-mediated killing, including the ability to switch from yeast to hyphal forms, which facilitates escape from phagocytosis, through membrane piercing *via* mechanical forces, or production of the hypha-associated toxin candidalysin [6,7]. Besides candidalysin, *Candida* secretes specific lipases, aspartyl proteinases (SAP-family proteins), and other hydrolytic enzymes responsible for immune host cell damage, favouring fungal dissemination or immune evasion [8].

Farnesol (FOH), a well-known quorum sensing molecules (QSMs) [9], has been implicated in modulating host immune responses by influencing immune cell activation, cytokine release, and neutrophil extracellular trap (NET) formation. Additionally, *C. albicans* actively remodels its cell wall composition in response to environmental stimuli, modulating the exposure of PAMPs to evade immune detection and phagocytosis.

Moreover, FOH has been implicated in several physiological processes, including filamentation, biofilm formation, drug efflux, and apoptosis [10,11]. Nevertheless, some evidence reports QSMs having an immunomodulatory effect on different immune cell morphotypes. In particular, FOH is likely to modulate host immune recognition in multiple ways, including the remodelling of β-glucan in response to alkaline pH [12]. Moreover, monocytes and neutrophils exposed to FOH display increased expression of activation markers and promote the release of proinflammatory cytokines, whereas the exposure of MΦs to E,*E*-FOH secreted by white cells stimulates their chemokinesis, improving migration towards the infection site [13,14]. Finally, FOH stimulates NETosis *via* Mac–1 and TLR2, activating a ROS-dependent NETosis pathway [15], confirming that it can mediate *Candida*-host communication.

Besides escaping from phagosomes, *C. albicans* also actively regulates the exposure of PAMPs (*i.e.*, β-1,3-glucan, mannans) by remodelling its cell wall in response to environmental stimuli, preventing the recognition and phagocytosis [16].

The tremendous ability of *C. albicans* to accommodate multiple environmental changes requires plasticity of chromatin structure and gene accessibility to transcriptional machinery, which is partially accomplished by epigenetic mechanisms. One of the most abundant and relevant post-translational modifications in *C. albicans* is the acetylation of H3K56 [17]. Such histone modification, which results from the activity of two enzymes, the acetyltransferases Rtt109 and the Hst3 deacetylase, contributes to fungal genome stability [17,18]. In a recent genome-wide analysis of H3K56ac, we highlighted its implication in regulating the transcription of genes involved in *C. albicans* morphological switching and, therefore, virulence [19].

In the present study, we investigated whether the acetylation of H3K56 might affect the *Candida*-MΦ interaction. Therefore, by means of the non-specific Hst3 inhibitor nicotinamide (NAM), we evaluated whether the alteration of H3K56 acetylation would affect the secretion of soluble factors by *C. albicans*. In particular, we tested the effect of *Candida* growth-conditioned media, treated or not with NAM, on murine MΦs at the morphological and functional levels. In addition, we

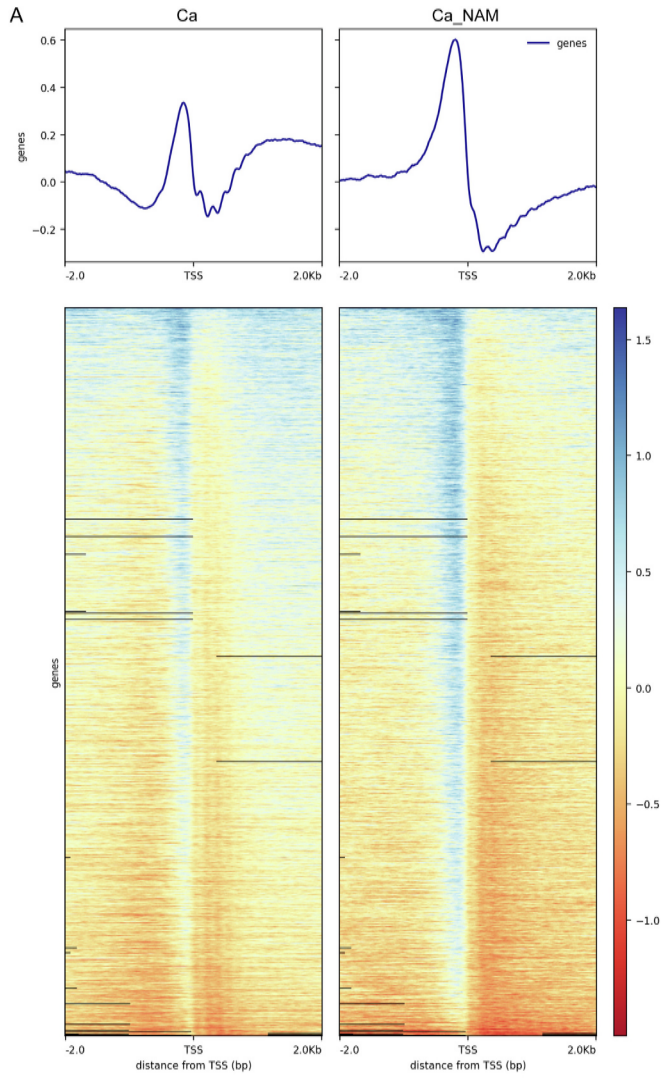


B

| Sample | Promoters [Peak nr] | Exons [Peak nr] | Intergenic [Peak nr] |
|---|---|---|---|
| Ca | 371 | 541 | 134 |
| Ca_NAM | 981 | 293 | 403 |

**Fig. 2.** H3K56 acetylation profiling in *C. albicans* following NAM treatment. A) Representative profile heatmap for H3K56ac ChIP-seq signal intensity around TSS (± 2kb) of RefSeq genes of control (Ca) and NAM-treated *C. albicans* (Ca_NAM). The gradient blue-to-red color indicates the high-to-low $\log_2$ ratio of the number of reads between the IP and the respective Input counts in the corresponding region. B) Number of significant peaks (FDR $\leq$ 0.05) from ChIP-seq analysis annotated in each genomic region.

analysed transcriptome modifications and genome enrichment of H3K56ac in *C. albicans* grown in the same experimental conditions to elucidate the involvement of this histone modification on the fungus virulence mechanisms.

## 2. Materials and methods

### 2.1. Chemicals

Nicotinamide (NAM) was purchased by Sigma-Aldrich (Milan, Italy). For all the experiments, 1 M NAM, freshly prepared in ultra-pure distilled water, was used as stock, filter-sterilized and added to culture media to obtain the required concentrations.

### 2.2. Western blot analysis and morphological evaluation of NAM-treated C. albicans

*C. albicans* wild-type strain SC5314 (ATCC-MYA-2876) was grown for approximately 48 h at 25 °C in YPD medium (1 % Yeast extract, 2 % Peptone, 2 % Dextrose). Subsequently, yeast cells were diluted to 0.1 OD (considering that 1 OD = 0.25 × $10^8$ cells/mL) in YPD fresh medium, and incubated at 25 °C for about 24 h. Then, yeasts were seeded onto 100 mm diameter Petri dishes at a density of 1.5 × $10^4$ cells/mL in 10 mL RPMI 1640 medium with 2 mM L-Glutamine (Euroclone, Pero, Italy) and incubated at 37 °C, 5 % $CO_2$ for 16 h. For NAM treatment, the stock solution was diluted at different concentrations (10, 25, 50 and 100 mM) in RPMI, and untreated *Candida* was used as control (Ca).

For Western blot analysis, Ca and Ca_NAM after 16 h of incubation were collected by centrifugation (4.700 *g*, 10 min at 4 °C) and resuspended in 10 mM EDTA, 10 mM Tris-HCl pH 7.4, 5 mM sodium butyrate, 5 mM NAM, 2.5 % 2-Mercaptoethanol and 10 % glycerol. Histone extraction was performed as described by Conte C. et al. [19]. For Western blotting, 0.5 μg of each histone sample was resolved by SDS-PAGE on 15 % polyacrylamide gel and transferred to a nitrocellulose membrane using the Trans-Blot Turbo Transfer System (Bio-Rad). The primary antibodies used were anti-H3 (Abcam) and anti-H3K56ac (Active Motif). The densitometric analysis was performed using ImageJ analysis software.

Brightfield optical microscopic images of *C. albicans* were taken at different time points (2, 4, 5, 6, 7, 9 and 16 h) by inverted microscopy (Zeiss Axiovert 5) coupled with a camera AxioCam 208 color (ZEISS, Germany) using 20× magnification and hyphal length was measured using Zeiss Zen 3.9 software. Cell density of untreated or NAM-treated *C. albicans* after 16 h of incubation was measured by ImageJ 1.49 software following this procedure: convert to 16-bit image➔process - find edges➔Image-adjust-threshold➔analyze Set measurements – tick "Area", "Area fraction", "Limit to threshold" "mean gray value", "Integrated density" and analyze and measure the area (%).

### 2.3. Macrophage viability

Murine macrophages J774A.1 cell line was supplied by LGC European partner of ATCC (LGC Standards) and cultured in RPMI 1640 (Euroclone, Pero, Italy) supplemented with 10 % fetal bovine serum (FBS, Euroclone, South America, origin EU approved), penicillin-streptomycin solution (100 μg/mL penicillin and 100 μg/mL streptomycin) (Euroclone, Italy).

The mitochondrial-dependent MTT [(3-(4,5-dimethylthiazol-2-yl)-2,5-diphenyl tetrazolium bromide] reduction to formazan was used to assess MΦs viability. Briefly, $10^5$ cells/well were seeded onto a 96-well plate (100 μL/each well) and incubated at 37 °C and 5 % $CO_2$ for 24 h with different concentrations of NAM: 10, 25, 50 and 100 mM. After 24 h, MTT was added at a final concentration of 0.5 mg/mL and incubated for 1 h at 37 °C. Then, the medium was discarded and 100 μL of DMSO were added to each well to dissolve formazan crystals. Cell viability was measured spectrophotometrically, reading the absorbance at 500 nm with reference at 620 nm.

### 2.4. RNA sequencing

For RNA extraction, *C. albicans* was grown first in YPD as described above (Section 2.2), and then 5.5 × $10^5$ cells /mL were inoculated in RPMI with or without 10 mM NAM for roughly 16 h, subsequently harvested (8.000 *g* for 10 min at 4 °C) and washed with UltraPure™ DNase/Rnase-Free Distilled Water (Thermo Fischer Scientific). The cell pellet was resuspended in 1 ml QIAzol Lysis Reagent (Qiagen) and disrupted mechanically with a BeadBug microtube homogeniser. Total RNA was purified following QIAzol manufacturer instructions. Three independent biological replicates were performed for either control or treated *C. albicans* cells. RNA quality was assessed with TapeStation

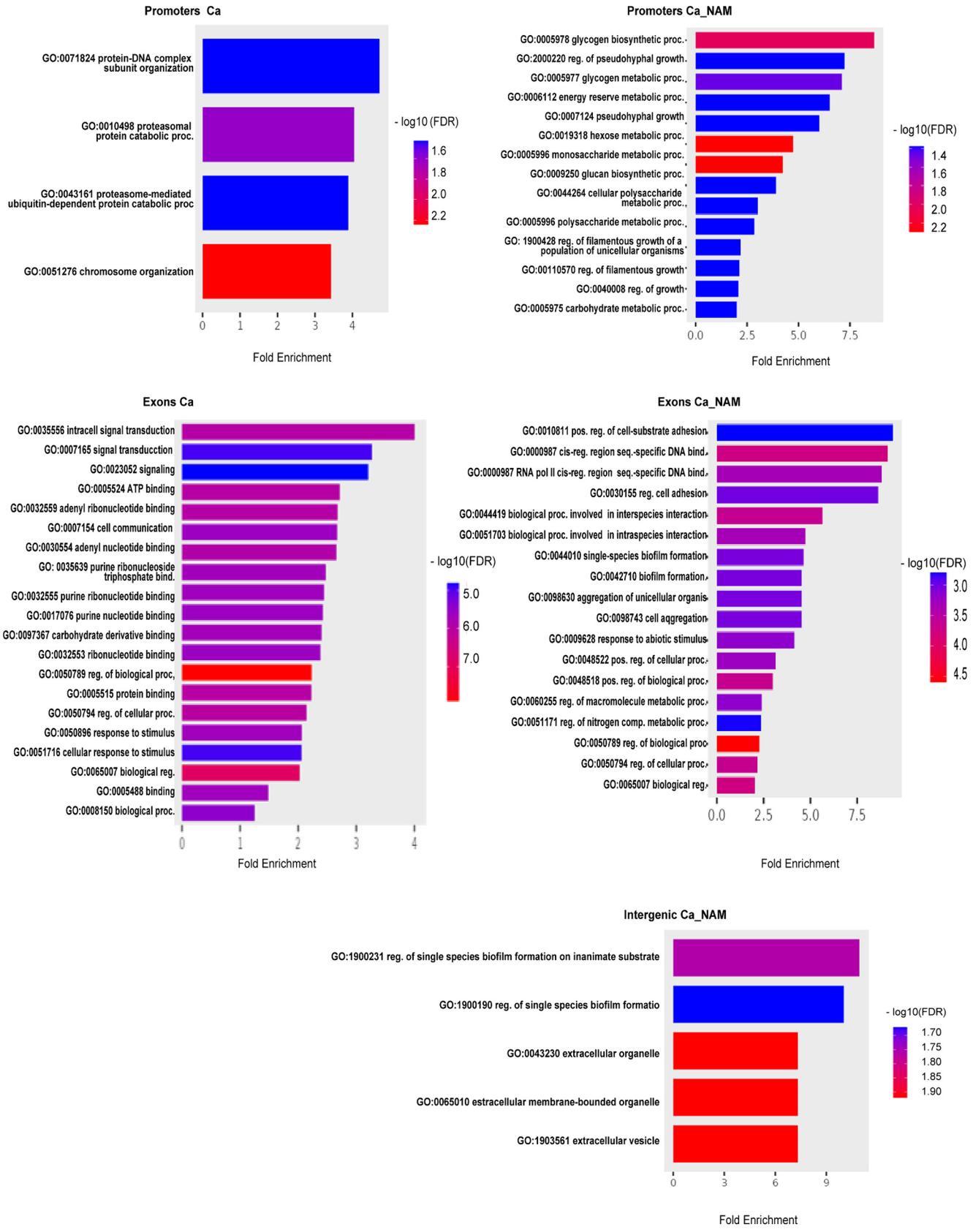


**Fig. 3.** Gene ontology enrichment analysis. Results of gene ontology analysis of ChIP-enriched regions in control (Ca) and NAM treated (Ca_NAM) cells performed for each genomic region (promoters, exons, intergenic) by ShinyGO 0.8. The analysis was conducted including all available gene sets with a pathway size minimum = 5 and FDR cutoff = 0.05.

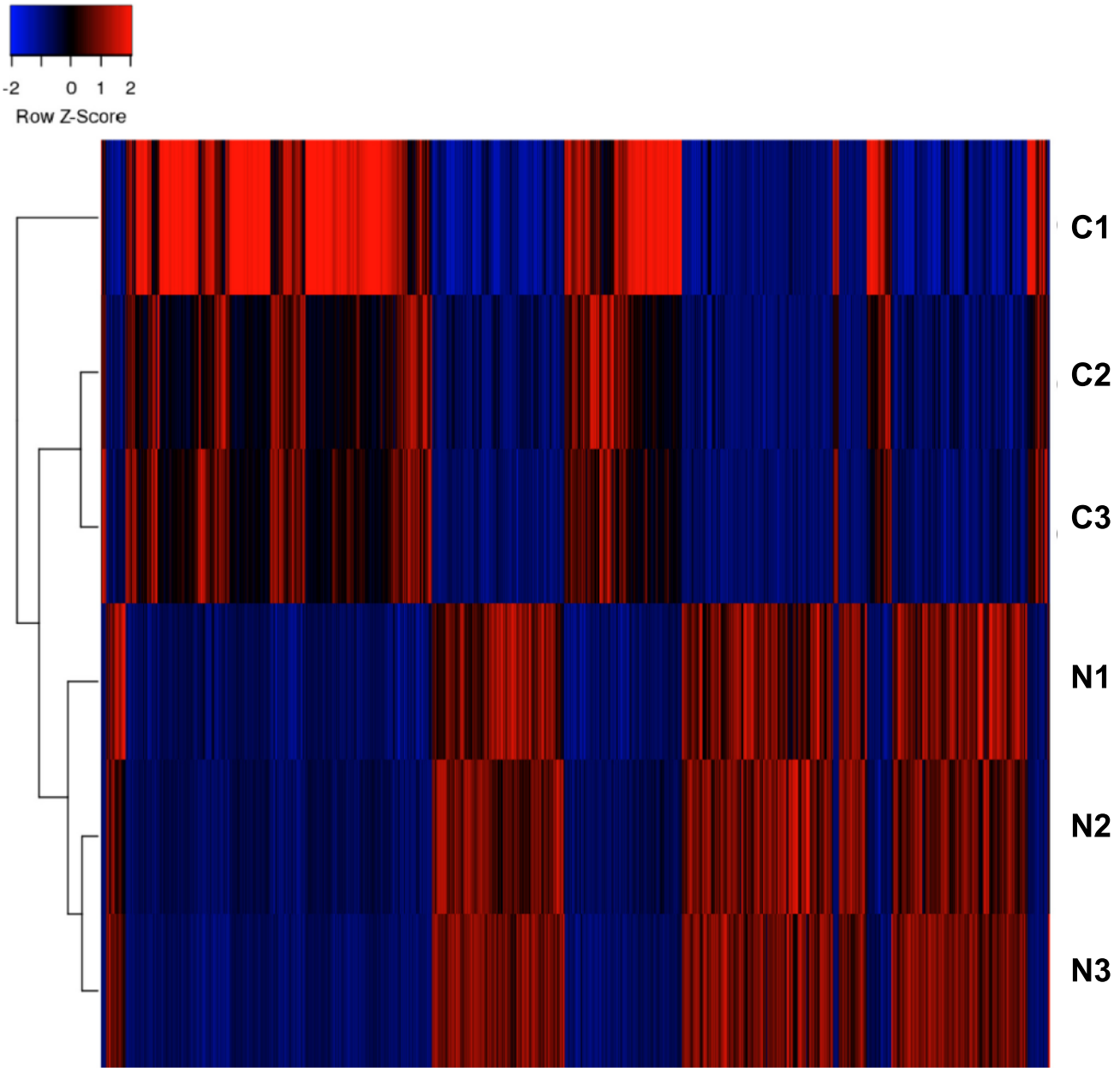


**Fig. 4.** Dysregulated genes following NAM treatment. Heatmap showing the expression levels in $\log_2$ RPKM+1 of differentially expressed genes among Ca (C) and Ca_NAM (N) (FDR $\leq$0.05). The experiment was performed in triplicate.

(Agilent) and only RNA with RIN $>$ 8 was used for RNA-seq library production.

For RNA sequencing, indexed libraries were prepared from 1 μg of purified RNA using TruSeq Stranded Total RNA Sample Prep Kit (Illumina Inc.), according to the manufacturer instructions. Libraries were pooled and sequenced (paired-end, 2 $\times$ 100 bp) on the NextSeq 550 platform (Illumina Inc.).

### 2.5. Chromatin immunoprecipitation of C. albicans

*C. albicans* was grown as described in Section 2.4. After 16 h at 37 °C, 5 % $CO_2$ *Candida* was cross-linked with 1 % formaldehyde for 15 min at RT with gentle shaking. The reaction was quenched by adding 125 mM glycine and incubating for 5 min at RT under gentle shaking. Chromatin immunoprecipitation was performed as previously described [20], except for cell lysis, which was carried out using a cryogenic freezer mill (SPEX SamplePrep 6970EFM Freezer/Mill). ChIP-seq libraries were generated from two independent biological replicates of H3K56ac and input following a previously published protocol [21] and sequenced on Illumina NextSeq 500 using 2 $\times$ 75 bp reads.

### 2.6. Bioinformatic analysis

For RNA sequencing, analysis was performed using the Flaski RNA-seq pipeline [22] and the reference strain *Candida albicans* SC5314 genome assembly GCA_000182965.3.

Data normalisation and differentially expressed transcripts were identified using DESeq2 with standard parameters. Genes with FDR $\leq$ 0.05 (False Discovery Rate) and with a value of Fold Change $\leq -1.5$ (for down-regulated genes) or Fold Change $\geq$1.5 (for up-regulated genes) were considered significantly differentially expressed. Expression levels are displayed in $\log_2$-transformed RPKM (Reads Per Kilobase of transcript per Million mapped reads).

For ChIP-sequencing, the analysis was performed using the Galaxy

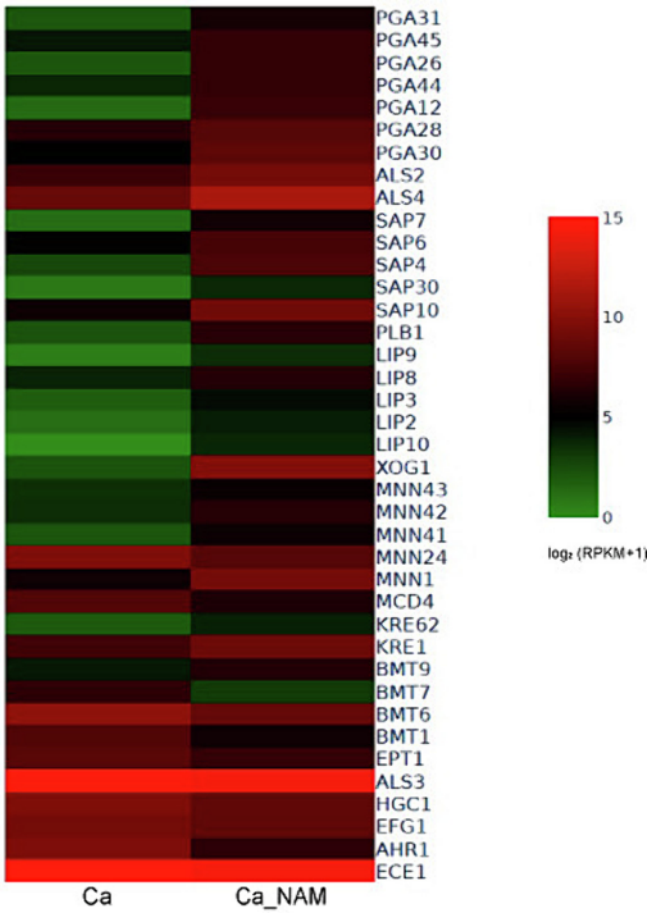


**Fig. 5.** NAM treatment leads to transcripts dysregulation of genes involved in virulence. Heatmaps showing the expression levels in $\log_2$ RPKM+1 of selected genes involved in glucans/mannans exposure, cell wall remodelling, and hydrolytic enzymes biosynthesis (FDR ≤0.05; distance measure: Euclidean; clustering algorithm: Ward).

tool [23].

Briefly, after FastQC quality check, the paired-end reads were aligned to the reference *Candida albicans* SC5314 genome (assembly GCA_000182965.3) using Bowtie 2 (Galaxy Version 2.4.4) and the generated BAM file was filtered with Filter BAM (Galaxy Version SAMTOOLS: 1.8). Mapped reads were indexed and merged using samtools MergeSamFiles (Galaxy Version 2.18.2.1) and converted to bigwig files using deepTools bamCoverage (Galaxy Version 3.5.1.0.0) with a bin size of 10 and normalisation to genomic content.

Peak calling was performed with MACS2 callpeak (Galaxy Version 2.2.7) using standard parameters for board regions. Peak annotation was carried out using annotatePeaks (Galaxy Version 4.11 + galaxy3).

Gene ontology analysis was performed by ShinyGO V0.80 [24] with following settings: Pathway database = all available gene sets; FDR cutoff = 0.05; min. pathway size = 5. All the protein−protein interaction (PPI) profiles were obtained from the STRING webserver (https://string-db.org/).

### 2.7. Preparation of C. albicans conditioned media

Conditioned media were obtained by growing *C. albicans* as described in 2.4 section. After 16 h, in RPMI and 5 % $CO_2$ at 37 °C with or without 10 mM NAM, culture media were collected, centrifuged at 10.000*g* for 10 min and filter sterilized using a 0.45 μm syringe filter. At the end of this procedure, we obtained the conditioned medium of *C. albicans* control (Ca-CM) and the conditioned medium of NAM-treated *C. albicans* (Ca_NAM-CM). Since NAM has low stability in water solution, to get the correct control media, RPMI with or without 10 mM NAM was incubated at 37 °C and 5 % $CO_2$ for 16 h and filter sterilized, obtaining the control medium (CTRL-M) and NAM-treated medium (NAM-M). All media were freshly prepared.

### 2.8. Phalloidin staining

To assay whether the morphology of J774A.1 cells was affected by *C. albicans* conditioned media, MΦs were stained with TRITC-Phalloidin after incubation with different conditioned media. In detail, J774A.1 cells were seeded on poly-lysine coated cover glasses at a density of 1.5 × $10^5$ cells/mL in 24-well plates, washed twice with PBS (Euroclone, Pero, Italy), exposed to CTRL-M, NAM-M, Ca-CM and Ca_NAM-CM, prepared as described in Section 2.6, and stained/imaged after 8 h of incubation.

After treatments, cells were fixed with 4 % paraformaldehyde for 5 min, washed and permeabilised with PBS-Triton X-100 (0.1 % v/v) for 10 min. Coverslips were then incubated with blocking buffer (1 % *w/v* BSA in PBS) for 30 min at RT and stained with 2 μg/mL TRITC-Phalloidin/ Hoechst 33342 for 1 h at room temperature (RT). Images were acquired by using a LEICA TCS SP8 confocal microscope.

The percentage of actin-bundle positive cells over the total, was calculated from multiple fields (each field = 30 cells), ensuring a total of 300 cells across various fields of view (and multiple coverslips) for each condition.

### 2.9. RTqPCR analysis of J774A.1

Total RNA was extracted using TRIzol reagent (Invitrogen, no. 15596018, New Zealand) following the manufacturer's instructions, and 500 ng of each RNA was retrotranscribed by M-MLV Reverse Transcriptase (GeneSpin S.r.l, Italy). The real-time PCR was performed using the QuantStudio™ 5 Real-Time PCR System (ThermoFisher). Different dilutions of cDNA were used for each gene in a 12 μL reaction using Luna Universal qPCR Master Mix (New England BioLabs, USA). The primer sequences are reported in supplementary material, Table S1. Results from three independent experiments in technical duplicates were analyzed using the Delta-Delta CT method and HPRT1 was used as a reference gene.

### 2.10. Quantitative analysis of farnesol by mass spectrometry

30 μL of each secretome sample from *Candida albicans*, treated or not with NAM 10 mM, were submitted to UPLC-ESI-MRM-MS analysis to quantify farnesol. Opportune blank samples of RPMI were also run. UPLC-ESI-MRM-MS analyses were performed on a 6500 Q-TRAP from Sciex equipped with Shimadzu LC-20A and Auto Sampler systems (Sciex). UPLC separation was performed on a Luna Omega Polar PS 1.6 μm C18 100 Å column (50 × 2.10 mm, Phenomenex) at a flow rate of 400 μL/min. 0.1 % Formic Acid in $H_2O$ (A) and 0.1 % Formic Acid in Acetonitrile (B) were used as mobile phases and the following gradient was performed: 0 % B from 0 to 4 min, 0 % to 95 % B over 10 min, then held at 95 % B for 5 min and re-equilibrated to 0 % B over 5 min. Q-TRAP 6500 was operated in positive MRM scanning mode, with declustering potential (DP) set at 30 V, entrance potential (EP) at 12 V, collision energy (CE) at 20 V and cell exit potential (CXP) at 12 V. Farnesol was monitored through the 205.0/149.0, 205.0/121.0 and 205.0/109.0 transitions: the area of peak related to the transition 205.0/121.0 was measured using the Analyst Software from Sciex and used for farnesol quantification in each sample. The other two transitions were used to confirm the occurrence of farnesol. An external calibration curve has been prepared using pure farnesol (Sigma-Aldrich, Merck Group) at concentrations ranging from 10 nM to 50 μM.

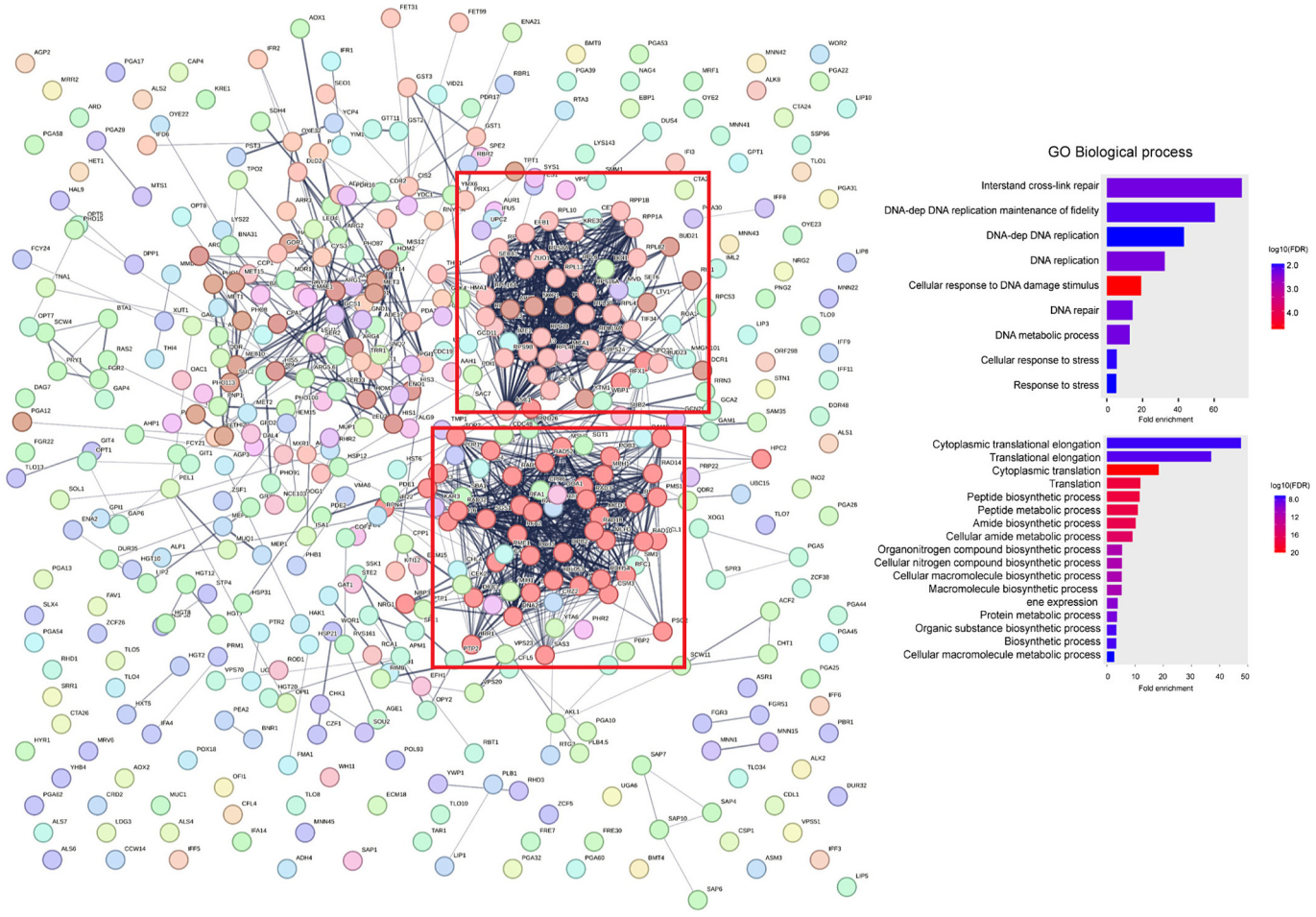


**Fig. 6.** STRING cluster analysis of genes upregulated in NAM-treated cells (FDR $\leq 0.05$). A Gene Ontology (GO) analysis was performed for the most relevant clusters (red squares), revealing an enrichment of proteins involved in gene expression regulation (clustering algorithm: MCL).

### *2.11. Statistical analysis*

Quantitative results are from at least three independent experiments and are expressed as means ± s.d. Data were statistically analyzed by the two-tailed Student *t*-test or, alternatively, one-way ANOVA with Dunnet's or Tukey's multiple comparison test by GraphPad Prism 7 (GraphPad Software). A *p*-value <0.05 was considered statistically significant.

## 3. Results

### *3.1. Inhibition of Hst3 impairs hyphae formation*

The modulation of morphogenesis is one of the most important skills used by *C. albicans* to respond to environmental changes and represents one of its main virulence factors. For instance, hyphae development is a strategy by which *C. albicans* escapes MΦs killing, inducing direct or indirect damage (*via* mechanical piercing or producing the candidalysin toxin) to the phagocyte membrane [7].

H3K56 acetylation is known to be involved in the yeast-to-hyphae transition. Indeed, the histone deacetylase Hst3 inhibition significantly impairs the formation of the hyphal crown around the macro-colonies on solid media and induces a V-shaped morphology under yeast-promoting conditions (YPD at 25 °C) [19]. Based on these results, we wondered whether the *Candida* morphological changes, following the modification of H3K56 acetylation, might be involved in the alteration and evasion of MΦs response.

To this aim, we first tested different concentrations of NAM (10–100 mM) to determine the minimum amount able to induce an accumulation of H3K56ac without compromising either *Candida* or MΦs viability. As previously seen for *Candida* grown in YPD at 25 °C [19], also in hyphae-promoting growth conditions (RPMI at 37 °C and 5 % $CO_2$), the concentration of 10 mM NAM was sufficient to favour a robust increment of H3K56 acetylation, confirmed by Western blotting of histones isolated from *Candida* after 16 h of treatment (Fig. 1A, B). The increased level of H3K56ac in NAM-treated cells (Ca_NAM), is associated with a less compact mycelium architecture, resulting in a lower cell density of approximately 38 ± 8 %, compared to 90 ± 1 % in untreated cells (Ca), thereby confirming the involvement of Hst3 in the yeast-to-hyphae transition (Fig. 1C). Interestingly, during the initial 5 h of growth in RPMI at 37 °C with 5 % $CO_2$, comparing Ca *vs* Ca_NAM, no significant differences were observed in germination or formation and elongation of pseudohyphae and hyphae. However, starting from 6 h of incubation, the hyphae of Ca_NAM were significantly shorter than those of Ca cells (Supp. Fig. 1), confirming the involvement of Hst3 in the yeast-to-hyphae transition (Fig. 1C). Moreover, 10 mM NAM did not affect MΦs viability and was chosen as the working concentration (Fig. 1D).

### *3.2. Genome-wide analysis of H3K56ac in C. albicans*

In order to identify H3K56ac-enriched genomic regions in *Candida* (Ca) and NAM-treated *Candida* (Ca_NAM), we performed a ChIP-seq analysis with an anti-H3K56ac antibody.

As shown in the plot profiles of Fig. 2A, a different distribution of H3K56 in genomic regions across the TSS of genes was observed among the control condition (Ca) and Ca_NAM. In particular, following NAM

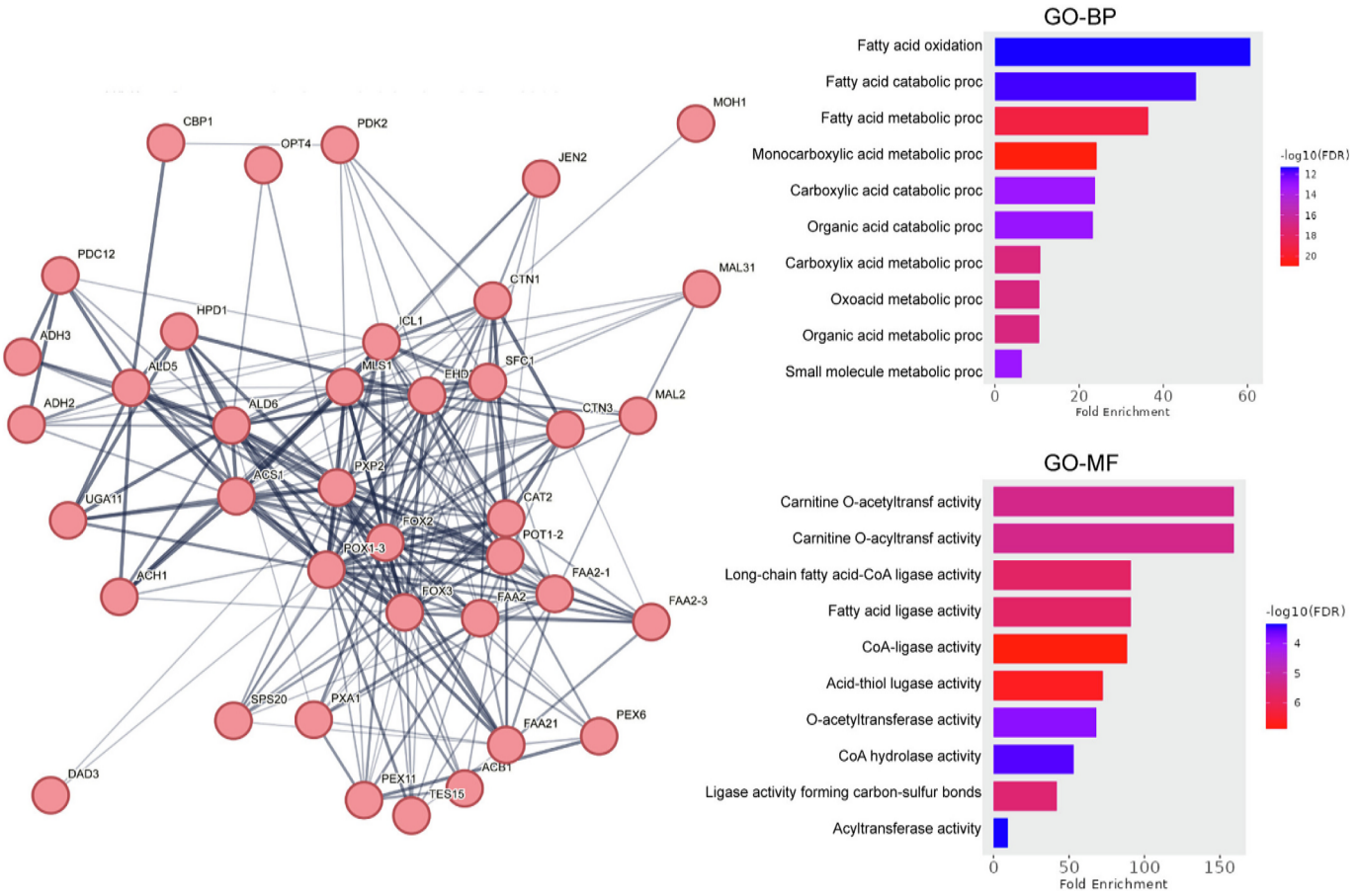


**Fig. 7.** STRING cluster analysis of genes downregulated in NAM-treated cells (FDR $\leq$ 0.05). Focus on the most relevant cluster 1, which includes 39 proteins (clustering algorithm: MCL). Biological processes (GO-BP) and molecular functions (GO-MF) enrichment analysis revealed an enrichment of terms related to acetyl-CoA processing (FDR $\leq$ 0.05).

treatment, a significant enrichment of K56 acetylated regions was observed predominantly in the promoters (Fig. 2B). Also, a higher number of peaks was found in intergenic regions, whereas a lower number was found in exons of NAM-treated compared to control cells (Fig. 2B).

To investigate more deeply the possible molecular mechanisms regulated by K56 acetylation/deacetylation, we performed a Gene Ontology (GO) analysis of ChIP-enriched regions in promoters, exons and intergenic both in control and NAM treated cells (Fig. 3).

The GO-analysis of ChIP-enriched regions mapping in promoters of control cells unveiled an enrichment of terms related to the proteasome and ubiquitin pathway, suggesting that in physiological conditions H3K56ac regulates the protein quality control mechanisms. Interestingly, the GO-analysis of the promoters ChIP-enriched regions in NAM treated cells, revealed a significant enrichment of terms related to sugar metabolisms, filamentation, and glucan biosynthetic processes. These results, not only highlight a central role of such histone modification in the basal metabolism of the fungus, but also confirm its potential involvement in phenotypic switching. Moreover, the enrichment of genes involved in glucan biosynthesis suggests a regulation of cell adhesion and an indirect impact on cell recognition by immune cells. Focusing on the exons, in not treated *C. albicans,* we found an enrichment of GO-terms relative to cell signalling and cell communication, ATP binding, purine nucleotide binding. By contrast, upon NAM treatment the terms mainly enriched were associated with cell adhesion, biological processes involved in intra- and inter- species interaction and biofilm formation. Notably, we observed a significant enrichment in the molecular functions named "cis-regulatory region sequence-specific DNA binding" and "RNA polymerase II cis-regulatory region sequence-specific DNA binding".

Finally, we did not find any GO-term significantly enriched in intergenic ChIP regions of control cells, whereas in NAM-treated cells we found an enrichment of terms related to biofilm formation and extracellular organelles.

### 3.3. *RNA sequencing unveils transcriptional dysregulation upon Hst3 inhibition*

To further elucidate the regulatory machinery dependent on H3K56ac, we compared the transcriptional profiles of Ca to Ca_NAM by RNA sequencing and found 958 up-regulated and 985 down-regulated genes (FDR $\leq$ 0.05) in samples exposed to NAM *vs.* control condition (Fig. 4).

Among them, a relevant dysregulation was observed in transcript abundance of genes involved in β-glucan and mannan exposure, cell wall proteins biosynthesis and hydrolytic secreted enzymes, including, for instance, mannosyltransferases (*i.e.*, *MNN1*, *MNN41* and *MNN43*), proteinases, phospholipases and lipases (*i.e.*, *SAP7*, *LIP3*, *PLB1*) and other enzymes that play a role in cell wall biosynthesis (*i.e.*, *PGA13*, *PGA26* and *PGA45*) (Fig. 5), supporting the hypothesis that the fluctuations of H3K56 acetylation might compromise expression of genes that interfere with the host-immune recognition and facilitate the host-immune escaping.

Among the downregulated genes, we identified *EFG1* (enhanced filamentous growth protein 1), a gene encoding for a transcription factor that has been implicated in several different regulatory networks,

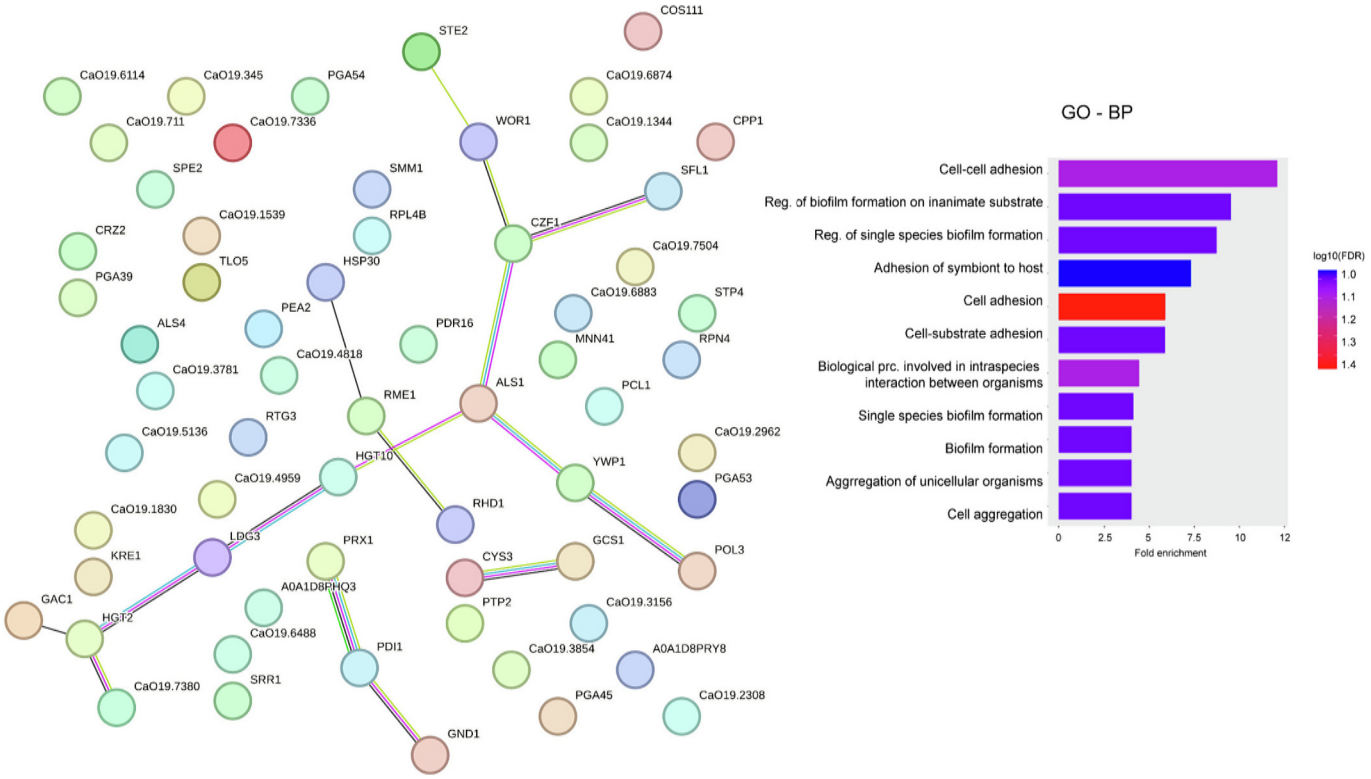


**Fig. 8.** STRING cluster analysis of genes transcriptionally upregulated and ChIP-enriched in NAM-treated cells (FDR $\leq$ 0.05). The most relevant cluster includes 12 proteins involved in phenotypic switching, cell adhesion and biofilm formation. Biological processes (GO-BP) enrichment analysis revealed an enrichment of terms related to cell adhesion.

including white/opaque switching, cell morphology, and biofilm formation [25]; *HGC1* (hypha-specific G1 cyclin-related protein 1), an essential gene for hyphal morphogenesis [26]; *AHR1* (Adhesion and hyphal regulator 1), a gene encoding a transcription factor which plays a crucial role in the activation of *ALS3* and *ECE1,* both involved in white-opaque switching, fungal adhesion and filamentation [27]; *EPT1*, coding for the enzyme responsible for the final step of phosphatidylethanolamine (PE) and phosphatidylcholine (PC) biosynthesis and reported to be overexpressed during hyphal elongation. Indeed, disruption of *EPT1,* causing a loss of PE and PC synthesis, leads to a reduced virulence of *C. albicans* [28] (Fig. 5).

To better analyze the processes regulated by H3K56ac, we performed a STRING and GO analysis. Among the up-regulated transcripts, we found two main large clusters, including 46 and 30 nodes of proteins involved in DNA replication and repair and translational processes (Fig. 6).

The analysis of the down-regulated transcripts revealed four clusters mainly including mitochondrial proteins as well as proteins involved in aminoacidic biosynthesis, ion transport, oxidation-reduction processes (Clusters 2, 3, 4, Supp. Figs. 2–4), TCA cycle, and, more generally, in biosynthesis, processing, and transport of acetyl-CoA (Cluster 1, Fig. 7). The latter is particularly interesting since it suggests a potential balance mechanism activated in response to NAM-induced hyperacetylation. Among others, a significant down-regulation was observed for the Acetyl-CoA hydrolase *ACH1*, the acyl-CoA oxidase *PXP2* responsible for the first step of acetyl-CoA biosynthesis from imported fatty acids [29], the fatty acid CoA ligases *FAA2-1*, *FAA2-3*, *FAA2* and *FAA21,* the Acyl-coenzyme A oxidase *POX1-3,* the major carnitine acetyltransferase *CAT2,* responsible for intracellular acetyl-CoA transport [30,31], the *ACS1* (Acetyl-coenzyme A synthetase 1) [32] and the pyruvate dehydrogenase kinase *PDK2* (Fig. 7). This result suggests that histone hyperacetylation following NAM treatment can induce a balance mechanism of Acetyl-CoA biosynthesis as already seen for HDAC inhibitors [33].

We already reported in Conte et al. 2022 that treatment of *C. albicans* with NAM, under yeast-promoting conditions (YPD; 25 °C), alters the expression of several virulence-related genes, primarily those related to filamentation, cell wall organization, and adhesion, leading to the formation of abnormal and enlarged filamentous structures called V-shaped hyphae.

As expected, comparing the RNA-seq results from Conte et al. 2022 with those derived from *C. albicans* grown under hypha-promoting conditions (RPMI; 37 °C; $CO_2$), we identified several common genes: 481 upregulated and 294 downregulated (Supp. Fig. 5).

### 3.4. Intersecting analysis of RNA-seq and ChIP-seq data

Intersecting RNA-seq and ChIP-seq results, we found 209 promoters, 70 exons and 101 intergenic regions whose H3K56 acetylation correlates with transcript dysregulation (Supp. Fig. 6). Among them, we focused our STRING and GO analysis on genes that displayed an accumulation of H3K56 acetylation upstream of the TSS upon NAM treatment and whose transcription was upregulated and thus considered directly regulated by this histone modification. We identified a cluster of 12 proteins (Fig. 8) such as: Als1 (Agglutinin-like protein 1) a cell surface adhesion protein which mediates both yeast-to-host tissue adherence and yeast aggregation [34]; Czf1 (Zinc cluster transcription factor 1) involved in the regulation of cell wall structure and also required for filament inhibition by farnesol [35,36]; Hgt2 (High-affinity Glucose Transporter) which is part of the core filamentation response network in *C. albicans* [37]; Wor1 (White-opaque regulator 1), a master regulator of white-opaque switching [38]; Ywp1, a yeast-specific protein that has been detected in the pseudohyphae [39], and has also been involved in processes such as biofilm dispersion and β-glucan masking control, consequently, its overexpression might have a role in limiting macrophage function. Overall, these results suggest that this histone modification is directly

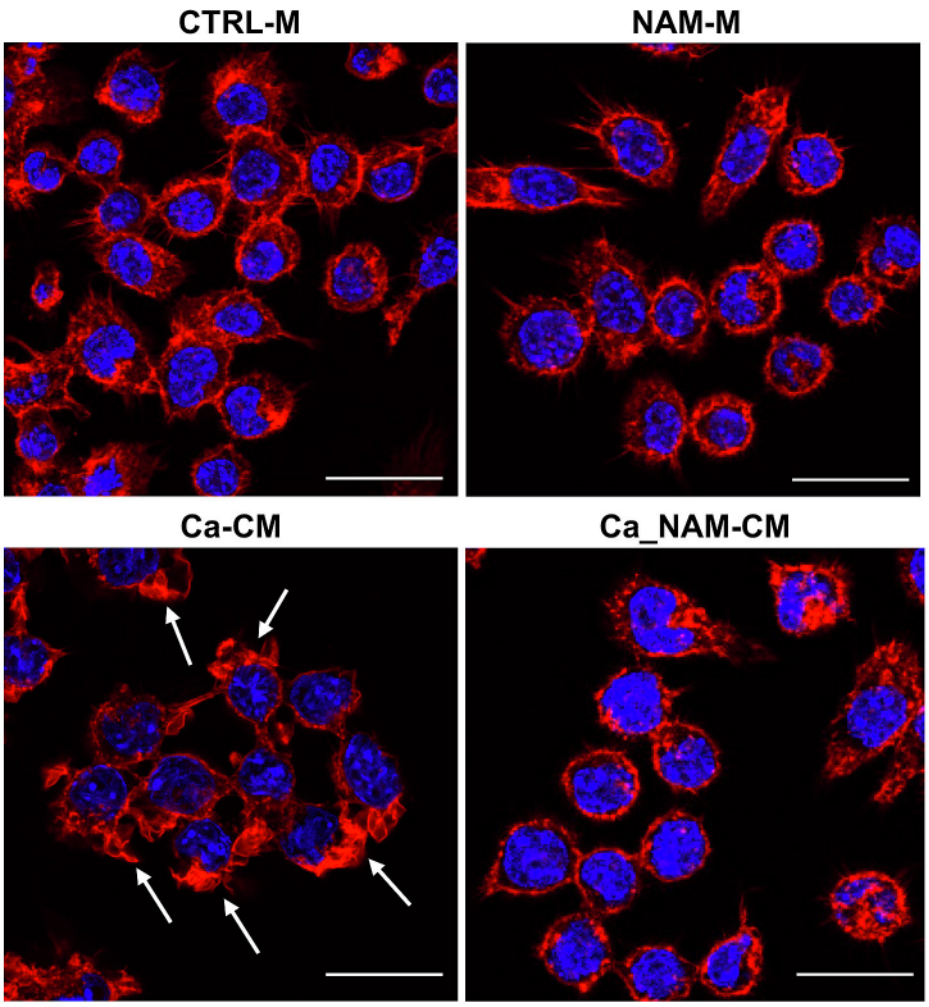


**Fig. 9.** NAM treatment reverts the ability of *C. albicans* conditioned medium to impair the cytoskeleton structure of J774A.1 cells. J774A.1 MΦs were exposed to filter-sterilized supernatants collected from *C. albicans* grown in RPMI medium (Ca-CM) or *C. albicans* grown in RPMI medium with 10 mM NAM (Ca_NAM-CM) and analyzed by confocal microscopy after 8 h of exposure following TRITC-phalloidin staining. Hoechst for nuclei (blue). Scale bar: 20 μm. CTRL-M and NAM-M indicate cells incubated with the two control media. White arrows indicate cells characterised by abnormal actin bundles. The experiment was performed in triplicate.

involved in the transcription rates of genes involved in phenotypic switching, cell adhesion and biofilm formation. This is consistent with the morphological observations that displayed a decrease in hyphae length and a loss of adhesiveness.

### 3.5. *C. albicans conditioned media affect MΦs morphology*

One of the immune escaping strategies adopted by *C. albicans* consists of secreting soluble factors that induce actin rearrangement in human epithelial and macrophage cells, impairing cytoskeletal functions [40,41]; therefore, we questioned whether H3K56 acetylation could be involved in regulating the secretion of these factors.

To this end, we investigated the effects of both conditioned media Ca-CM and Ca_NAM-CM on J774A.1 MΦs. As negative control media, we used CTRL-M and NAM-M, respectively RPMI medium and RPMI medium supplemented with 10 mM NAM, both incubated for 16 h at 37 °C, 5 % $CO_2$.

J774A.1 MΦs were incubated for 8 h with each of these conditioned media, and their cytoskeletal morphology was monitored by confocal microscopy following TRITC-phalloidin staining. Stimulation with Ca-CM induced in 48 ± 15 % of cells a peculiar phenotype characterised by cells with unusual actin bundles compared to the other experimental conditions; in particular, actin-rich protrusions seem to be shorter and less structured compared to CTRL-M, suggesting that *Candida* secretes soluble factors that impair actin polymerisation in MΦs (Fig. 9).

On the other hand, MΦs incubated with Ca_NAM-CM showed a morphological phenotype similar to those with CTRL-M and NAM-M, suggesting that the accumulation of the H3K56 acetylation in *Candida* reduces the production and/or secretion of metabolites responsible for the appearance of actin bundles in MΦs (Fig. 9).

### 3.6. *C. albicans conditioned media affect macrophage response*

To better investigate the different MΦ responses, we analyzed a panel of pro- and anti-inflammatory cytokines by RTqPCR in J774A.1 cells exposed for 8 h to the above mentioned media (Fig. 10). As expected, MΦs sensed the Ca-CM by significantly inducing cytokine expression; on the contrary, the response of MΦs post-incubation with Ca_NAM-CM was limited. The differential cytokine stimulation by the two conditioned media suggests that Hst3 inhibition profoundly alters the production and release of PAMPs and their subsequent recognition by PRRs, followed by cytokine production. Therefore, when Hst3 works properly, and H3K56 acetylation is not altered, *Candida* seems to release factors that i) alter actin polymerisation and remodelling processes of MΦs and, at the same time, ii) stimulate cytokine production for the recruitment of other immune cells and the promotion of the indirect killing.

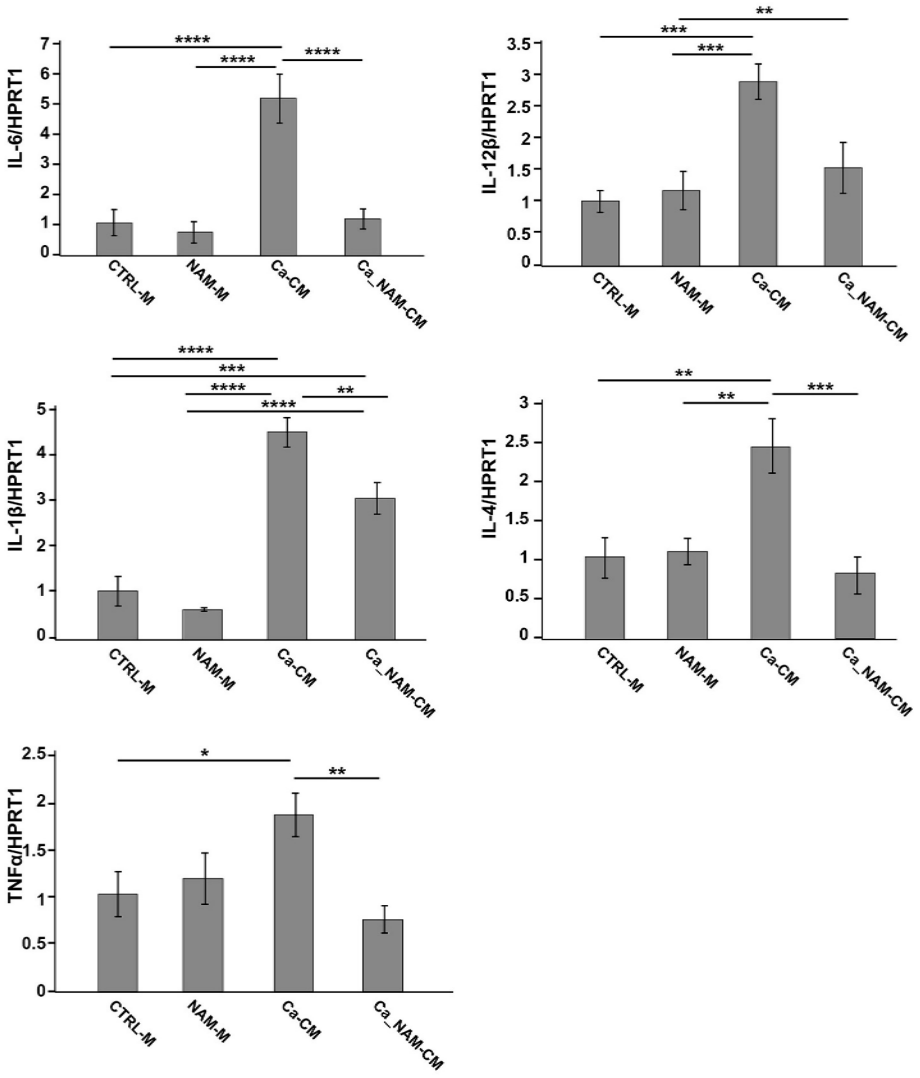


**Fig. 10.** NAM-treated *Candida* conditioned medium partially stimulates cytokine response. The indicated cytokines were analyzed by RTqPCR in J774A.1 cells exposed to filter-sterilized supernatants collected from *C. albicans* grown in RPMI medium (Ca-CM) or *C. albicans* grown in RPMI medium with 10 mM NAM (Ca_NAM-CM) for 8 h. MΦs incubated with just medium (CTRL-M) or NAM (NAM-M) were used as negative controls. HPRT1 was used as a housekeeping gene. Data are expressed as the mean ± s.d. of three independent experiments (one-way ANOVA with Tukey's test, **p*-value ≤0.05, **p-value ≤0.01, ***p-value ≤0.001, ***p-value ≤0.0001), and the mean of controls was set to 1.

### *3.7. Farnesol production increases upon Hst3 inhibition*

Several studies have suggested that QSMs can induce complex cellular behaviour, including morphological switches and secretion of extracellular enzymes. In particular, FOH, the first characterised QSM in fungi, has been shown to inhibit the yeast-to-mycelium transition of *C. albicans* [10–42]. Therefore, we wondered whether H3K56 acetylation could affect FOH production.

To this end, we collected *C. albicans* conditioned media after 16 h of growth at 37 °C, 5 % $CO_2$ in RPMI, alternatively with or without 10 mM NAM in order to have a *C. albicans* conditioned medium (Ca-CM) and a NAM-treated *C. albicans* conditioned medium (Ca_NAM-CM). Afterwards, we quantified the most representative QSM by mass spectrometry in both conditioned media. As shown in Fig. 11, FOH was significantly higher in the medium collected from *C. albicans* grown upon Hst3 inhibition (Ca_NAM-CM) compared to the control supernatant (Ca-CM), suggesting that the production of this QSM is directly or indirectly affected by H3K56 acetylation. Indeed, this result is in agreement with the already documented ability of FOH to inhibit the yeast-to-hypha transition [10–42] and with the result reported in Fig. 1C, where *Candida* treated with NAM showed an impaired hyphae formation.

## 4. Discussion

*Candida albicans* is an important human pathogen whose virulence factors confer extreme plasticity and the ability to survive in different anatomical sites, each with its own specific set of environmental pressures. Among the virulence factors, the reversible transition between unicellular yeast cells and filamentous forms has been linked to the H3K56 acetylation, regulated by the histone acetyltransferase Rtt109 and the histone deacetylase Hst3 [19–43]. Several known HDAC inhibitors have already been investigated as potential new antifungal therapies, but the selectivity of these compounds remains a significant issue [43]. In Conte et al. 2022, we tested three of the currently available sirtuin inhibitors (Inauhzin, Sirtinol, and SirReal2), but none of them exhibited activity against Hst3p. Therefore, NAM was used as a non-specific sirtuin inhibitor to explore the effects of H3K56ac accumulation on *Candida* grown under yeast-promoting conditions (in YPD at 25 °C) [19]. In the present study, we explored the biological

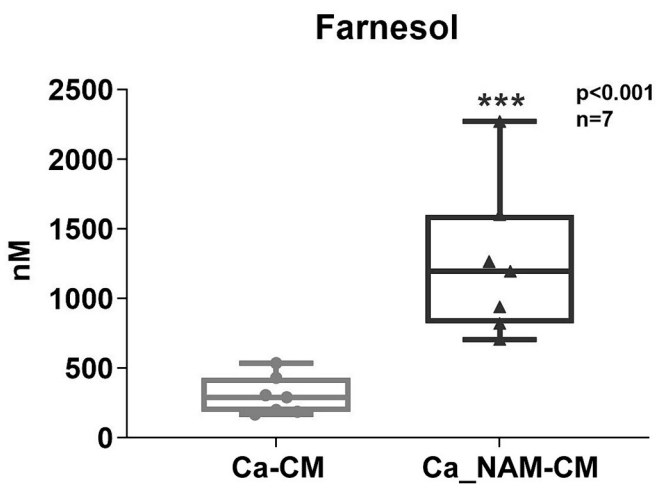


**Fig. 11.** Farnesol content is higher under Hst3 inhibition. The content of FOH in the Ca-CM and Ca_NAM-CM was quantified by mass spectrometry analysis. Values are the mean ± s.d. of seven independent experiments, *** $p < 0.001$ (*t*-test).

consequence of NAM treatment on *Candida* in hyphae-promoting conditions (RPMI at 37 °C and 5 % $CO_2$). In each growth condition, inhibition of Hst3 causes morphological changes; in particular, in the first case, it induces an abnormal phenotype called V-shaped hyphae, while in the second case, it slows down hyphal elongation.

As already extensively reported, the ability to rapidly switch between yeast and filamentous forms is one of the many strategies enrolled by *Candida* to escape host recognition and invade the host organism, including changes in adhesion properties, antigen expression, and tissue affinities [44]. During all these virulence processes, several proteins are secreted through the classical and/or non-canonical secretory pathway, including secreted aspartyl proteases and phospholipases, whose interaction and consequent effect on host cells help to prevent or limit the extent of clearance by the host immune system. Starting from this, we wondered if Hst3 could affect, in addition to hyphal growth, also the production of virulence-associated soluble factors able to modulate *Candida*-host interaction.

Our findings highlight that the correct functioning of Hst3 leads to the production and/or secretion of soluble factors that impair the actin polymerisation in MΦs, causing a peculiar phenotype characterised by unusual actin bundles and shorter actin-rich protrusions, which could likely limit the phagocytic activity of MΦs. Indeed, in order to eliminate the invading organism, phagocytosis requires actin cytoskeletal remodelling, leading to distinct F-actin-rich membrane structures. The macrophage filopodia sense the microenvironment, direct cell migration and once found the pathogen, surround it, assuming the typical morphology of a cup [45]. The actin cytoskeleton changes of MΦs incubated with the conditioned medium from *Candida* control clearly revealed a resistance mechanism of *C. albicans* to macrophage killing and confirm how the host-pathogen interaction can determine the evolution to different diseases.

On the contrary, the accumulation of the H3K56 acetylation in *Candida* alters the composition of the conditioned medium, without impairing the actin polymerisation of MΦs and stimulating less efficiently cytokine expression, particularly of IL-6, IL-12b, IL-4 and TNFα, in MΦs.

By mass spectrometry analysis, we found that FOH, the most known Quorum-Sensing molecule, was significantly more abundant in medium from NAM-treated *C. albicans*, suggesting that hyperacetylation of H3K56 might be involved in the production and release of this QSM. QSMs are considered key players in modulating immune cell response; in particular, FOH seems to control macrophage migration both *in vitro* and *in vivo*, as well as *C. albicans* filamentation [15]. The higher content of FOH in NAM-treated conditioned medium might account for the defective hyphal elongation and, at the same time, for the limited cytokine production of MΦs post-exposure to the medium. Indeed, according to Navarathna et al., exogenous FOH interferes with cytokine expression during candidiasis in a mouse model [46].

To deeply understand how the alteration of the acetylation level of H3K56 can affect *C. albicans* virulence mechanisms, we performed a ChIP-seq and an RNA-seq analysis.

Focusing on genes directly regulated by H3K56 acetylation, we selected transcriptionally up-regulated genes that showed ChIP-enriched regions upon NAM treatment. STRING and Gene Ontology analyses revealed that many of the ChIP-enriched genomic regions are related to phenotypic switching regulation, cell adhesion and biofilm formation.

Moreover, among the genes directly regulated by this epigenetic modification, there are different genes associated with the cell surface and for this reason possibly involved in the release of soluble factors, such as some GPI-anchored cell wall proteins (PGA39, PGA45, PGA53, PGA54) and some other directly involved in cell wall protein mannosylation (MNN41), sphingolipid homeostasis (RTG3) and lipid metabolism (RPN4).

Supporting this hypothesis, many other genes indirectly controlled by H3K56 acetylation that came out from the RNA-seq analysis are hydrolytic secreted enzymes like proteinases, phospholipases and lipases (*i.e.*, *SAP7*, *LIP3*, *PLB1*).

Among the indirectly regulated genes, of note, is the presence of some genes involved in the biosynthesis, processing, and transport of acetyl-CoA, suggesting that a balance mechanism might be activated in response to the hyperacetylation induced by NAM treatment, in line with the phenotype triggered by HDAC inhibitors, which lead to acetyl-CoA depletion and consequent lethal metabolic stress [33].

Although NAM is a non-specific inhibitor of sirtuins, and may potentially affect other cellular processes, the significant increase in H3K56ac levels after NAM treatment, together with our RNA-seq and ChIP-seq data, highlights the critical role of H3K56 acetylation in *Candida* virulence. Our data confirm that Hst3 is a promising target for the development of novel antifungal therapies.

## 5. Conclusions

When Hst3 works properly, it profoundly affects the production and/or release of PAMPs, which, following their recognition by PRR on MΦs, compromise actin remodelling; at the same time, the PAMPs-containing conditioned medium is sensed by MΦs which in turn produce and release pro-inflammatory cytokines attracting other immune cells aimed to kill the invading fungus.

Altogether, our data emphasize the pleiotropic effect of the epigenetic fluctuation of H3K56 acetylation and are consistent with the Hst3 role in connecting several pathways involved in different processes, survival and virulence mechanisms enrolled by *C. albicans*.

## Funding

This work was supported by the University of Salerno intramural funds FARB.

## CRediT authorship contribution statement

**Daniela Eletto:** Writing – review & editing, Methodology, Investigation, Data curation. **Martina Pannetta:** Methodology, Investigation. **Roberta Esposito:** Methodology, Investigation. **Maria Chiara Monti:** Writing – original draft, Software, Methodology, Investigation. **Elva Morretta:** Methodology, Investigation. **Peter Tessarz:** Writing – review & editing, Methodology, Investigation, Data curation. **Silvana Morello:** Writing – review & editing, Investigation, Data curation. **Alessandra Tosco:** Writing – review & editing, Validation, Investigation, Funding

acquisition, Data curation, Conceptualization. **Amalia Porta:** Writing – review & editing, Writing – original draft, Visualization, Validation, Supervision, Investigation, Funding acquisition, Data curation, Conceptualization.

## Declaration of competing interest

The authors declare that they have no known competing financial interests or personal relationships that could have influenced the work described in this paper.

## Data availability

The datasets presented in this study can be found in the ArrayExpress database at EMBL-EBI (www.ebi.ac.uk/arrayexpress) under accession numbers: E-MTAB-13348 (RNA-seq); E-MTAB-13387 (ChIP-seq).

## Acknowledgments

Not applicable.

## Appendix A. Supplementary data

Supplementary data to this article can be found online at https://doi.org/10.1016/j.bbagrm.2024.195048.

## References

[1] F.L. Mayer, D. Wilson, B. Hube, *Candida albicans* pathogenicity mechanisms, Virulence 4 (2) (2013) 119–128, https://doi.org/10.4161/viru.22913.
[2] J. Talapko, M. Juzbašić, T. Matijević, E. Pustijanac, S. Bekić, I. Kotris, I. Škrlec, Candida albicans-the virulence factors and clinical manifestations of infection, J Fungi (Basel) 7 (2) (2021) 79, https://doi.org/10.3390/jof7020079.
[3] P. Godoy, P.J. Darlington, M. Whiteway, Genetic screening of Candida albicans inactivation mutants identifies new genes involved in macrophage-fungal cell interactions, Front. Microbiol. 13 (2022) 833655, https://doi.org/10.3389/fmicb.2022.833655.
[4] M.G. Netea, N.A. Gow, C.A. Munro, S. Bates, C. Collins, G. Ferwerda, R.P. Hobson, G. Bertram, H.B. Hughes, T. Jansen, L. Jacobs, E.T. Buurman, K. Gijzen, D. L. Williams, R. Torensma, A. McKinnon, D.M. MacCallum, F.C. Odds, J.W. Van der Meer, A.J. Brown, B.J. Kullberg, Immune sensing of Candida albicans requires cooperative recognition of mannans and glucans by lectin and Toll-like receptors, J. Clin. Invest. 116 (6) (2006) 1642–1650, https://doi.org/10.1172/JCI27114.
[5] L.A. Perez-Garcia, D.F. Diaz-Jimenez, A. Lopez-Esparza, H.M. Mora-Montes, Role of cell wall polysaccharides during recognition of Candida albicans by the innate immune system, J Glycobiology 1 (2011) 102.
[6] J.M. Bain, J. Louw, L.E. Lewis, B. Okai, C.A. Walls, E.R. Ballou, L.A. Walker, D. Reid, C.A. Munro, A.J. Brown, G.D. Brown, N.A. Gow, L.P. Erwig, Candida albicans hypha formation and mannan masking of β-glucan inhibit macrophage phagosome maturation, mBio 5 (6) (2014) e01874, https://doi.org/10.1128/mBio.01874-14.
[7] L. Kasper, A. König, P.A. Koenig, M.S. Gresnigt, J. Westman, R.A. Drummond, M. S. Lionakis, O. Groß, J. Ruland, J.R. Naglik, B. Hube, The fungal peptide toxin Candidalysin activates the NLRP3 inflammasome and causes cytolysis in mononuclear phagocytes, Nat Commun. 9 (1) (2018) 4260. Published 2018 Oct 15, https://doi.org/10.1038/s41467-018-06607-1.
[8] H. Wu, D. Downs, K. Ghosh, A.K. Ghosh, P. Staib, M. Monod, J. Tang, Candida albicans secreted aspartic proteases 4-6 induce apoptosis of epithelial cells by a novel Trojan horse mechanism, FASEB J. 27 (6) (2013) 2132–2144, doi:10.1096/fj.12-214353. PMID: 23430844; PMCID: PMC6188231.
[9] J.M. Hornby, E.C. Jensen, A.D. Lisec, J.J. Tasto, B. Jahnke, R. Shoemaker, P. Dussault, K.W. Nickerson, Quorum sensing in the dimorphic fungus Candida albicans is mediated by farnesol, Appl. Environ. Microbiol. 67 (7) (2001) 2982–2992, https://doi.org/10.1128/AEM.67.7.2982-2992.2001.
[10] N.E. Egbe, Dornelles TO, C.M. Paget, L.M. Castelli, M.P. Ashe, Farnesol inhibits translation to limit growth and filamentation in *C. albicans* and *S. cerevisiae*, Microb Cell. 4 (9) (2017) 294–304, https://doi.org/10.15698/mic2017.09.589 (PMID: 28913344; PMCID: PMC5597792).
[11] G. Ramage, S.P. Saville, B.L. Wickes, J.L. López-Ribot, Inhibition of Candida albicans biofilm formation by farnesol, a quorum-sensing molecule, Appl. Environ. Microbiol. 68 (11) (2002) 5459–5463, doi:10.1128/AEM.68.11.5459-5463.2002. PMID: 12406738; PMCID: PMC129887.
[12] F. Cottier, S. Sherrington, S. Cockerill, Toledo V. Del Olmo, S. Kissane, H. Tournu, L. Orsini, G.E. Palmer, J.C. Pérez, R.A. Hall, Remasking of *Candida albicans* β-glucan in response to environmental pH is regulated by quorum sensing, mBio 10 (5) (2019), https://doi.org/10.1128/mBio.02347-19 e02347-19.
[13] I. Leonhardt, S. Spielberg, M. Weber, D. Albrecht-Eckardt, M. Bläss, R. Claus, D. Barz, K. Scherlach, C. Hertweck, J. Löffler, K. Hünniger, O. Kurzai, The fungal quorum-sensing molecule farnesol activates innate immune cells but suppresses cellular adaptive immunity, mBio 6 (2) (2015) e00143, https://doi.org/10.1128/mBio.00143-15.
[14] J.C. Hargarten, T.C. Moore, T.M. Petro, K.W. Nickerson, A.L. Atkin, Candida albicans quorum sensing molecules stimulate mouse macrophage migration, Infect. Immun. 83 (10) (2015) 3857–3864, https://doi.org/10.1128/IAI.00886-15.
[15] M. Zawrotniak, K. Wojtalik, M. Rapala-Kozik, Farnesol, a quorum-sensing molecule of Candida albicans triggers the release of neutrophil extracellular traps, Cells 8 (12) (2019) 1611, https://doi.org/10.3390/cells8121611.
[16] L.J. de Assis, J.M. Bain, C. Liddle, I. Leaves, C. Hacker, R. Peres da Silva, R. Yuecel, A. Bebes, D. Stead, D.S. Childers, A. Pradhan, K. Mackenzie, K. Lagree, D. E. Larcombe, Q. Ma, G.M. Avelar, M.G. Netea, L.P. Erwig, A.P. Mitchell, G. D. Brown, N.A.R. Gow, A.J.P. Brown, Nature of β-1,3-glucan-exposing features on Candida albicans cell wall and their modulation, mBio 13 (6) (2022) e0260522, https://doi.org/10.1128/mbio.02605-22.
[17] I. Celic, H. Masumoto, W.P. Griffith, P. Meluh, R.J. Cotter, J.D. Boeke, A. Verreault, The sirtuins hst3 and Hst4p preserve genome integrity by controlling histone h3 lysine 56 deacetylation, Curr. Biol. 16 (13) (2006) 1280–1289, https://doi.org/10.1016/j.cub.2006.06.023.
[18] H. Wurtele, S. Tsao, G. Lépine, A. Mullick, J. Tremblay, P. Drogaris, E.H. Lee, P. Thibault, A. Verreault, M. Raymond, Modulation of histone H3 lysine 56 acetylation as an antifungal therapeutic strategy, Nat. Med. 16 (7) (2010) 774–780, https://doi.org/10.1038/nm.2175.
[19] M. Conte, D. Eletto, M. Pannetta, A.M. Petrone, M.C. Monti, C. Cassiano, G. Giurato, F. Rizzo, P. Tessarz, A. Petrella, A. Tosco, A. Porta, Effects of Hst3p inhibition in Candida albicans: a genome-wide H3K56 acetylation analysis, Front. Cell. Infect. Microbiol. 12 (2022) 1031814, https://doi.org/10.3389/fcimb.2022.1031814.
[20] J.S.P. Mawer, J. Massen, C. Reichert, N. Grabenhorst, C. Mylonas, P. Tessarz, Nhp2 is a reader of H2AQ105me and part of a network integrating metabolism with rRNA synthesis, EMBO Rep. 22 (10) (2021) e52435, https://doi.org/10.15252/embr.202152435.
[21] E. Ford, C. Nikopoulou, A. Kokkalis, D. Thanos, A method for generating highly multiplexed ChIP-seq libraries, BMC. Res. Notes 7 (2014) 312, https://doi.org/10.1186/1756-0500-7-312.
[22] A. Iqbal, C. Duitama, F. Metge, D. Rosskopp, J. Boucas, Flaski (2021), https://doi.org/10.5281/zenodo.4849515.
[23] E. Afgan, D. Baker, B. Batut, M. van den Beek, D. Bouvier, M. Cech, J. Chilton, D. Clements, N. Coraor, B.A. Grüning, A. Guerler, J. Hillman-Jackson, S. Hiltemann, V. Jalili, H. Rasche, N. Soranzo, J. Goecks, J. Taylor, A. Nekrutenko, D. Blankenberg, The galaxy platform for accessible, reproducible and collaborative biomedical analyses: 2018 update, Nucleic Acids Res. 46 (W1) (2018) W537–W544, https://doi.org/10.1093/nar/gky379.
[24] S.X. Ge, D. Jung, R. Yao, ShinyGO: a graphical gene-set enrichment tool for animals and plants, Bioinformatics 36 (8) (2020) 2628–2629, https://doi.org/10.1093/bioinformatics/btz931.
[25] V.E. Glazier, EFG1, everyone's favorite gene in Candida albicans: a comprehensive literature review, Front. Cell. Infect. Microbiol. 12 (2022) 855229, https://doi.org/10.3389/fcimb.2022.855229.
[26] X. Zheng, Y. Wang, Y. Wang, Hgc1, a novel hypha-specific G1 cyclin-related protein regulates Candida albicans hyphal morphogenesis, EMBO J. 23 (8) (2004) 1845–1856, https://doi.org/10.1038/sj.emboj.7600195.
[27] S. Ruben, E. Garbe, S. Mogavero, D. Albrecht-Eckardt, D. Hellwig, A. Häder, T. Krüger, K. Gerth, I.D. Jacobsen, O. Elshafee, S. Brunke, K. Hünniger, O. Kniemeyer, A.A. Brakhage, J. Morschhäuser, B. Hube, S. Vylkova, O. Kurzai, R. Martin, Ahr1 and Tup1 contribute to the transcriptional control of virulence-associated genes in Candida albicans, mBio 11 (2) (2020) e00206-20, https://doi.org/10.1128/mBio.00206-20.
[28] R.N. Tams, C.D. Cassilly, S. Anaokar, W.T. Brewer, J.T. Dinsmore, Y.L. Chen, J. Patton-Vogt, T.B. Reynolds, Overproduction of phospholipids by the Kennedy pathway leads to Hypervirulence in *Candida albicans*, Front. Microbiol. 10 (2019) 86, https://doi.org/10.3389/fmicb.2019.00086.
[29] K. Okazaki, H. Tan, S. Fukui, I. Kubota, T. Kamiryo, Peroxisomal acyl-coenzyme A oxidase multigene family of the yeast Candida tropicalis; nucleotide sequence of a third gene and its protein product, Gene 58 (1) (1987) 37–44.
[30] K. Strijbis, C.W. van Roermund, J. van den Burg, M. van den Berg, G.P. Hardy, R. J. Wanders, B. Distel, Contributions of carnitine acetyltransferases to intracellular acetyl unit transport in Candida albicans, J. Biol. Chem. 285 (32) (2010) 24335–24346, https://doi.org/10.1074/jbc.M109.094250.
[31] K. Strijbis, C.W. van Roermund, W.F. Visser, E.C. Mol, J. van den Burg, D. M. MacCallum, F.C. Odds, E. Paramonova, B.P. Krom, B. Distel, Carnitine-dependent transport of acetyl coenzyme A in Candida albicans is essential for growth on nonfermentable carbon sources and contributes to biofilm formation, Eukaryot. Cell 7 (4) (2008) 610–618, https://doi.org/10.1128/EC.00017-08.
[32] A.J. Carman, S. Vylkova, M.C. Lorenz, Role of acetyl coenzyme A synthesis and breakdown in alternative carbon source utilization in Candida albicans, Eukaryot. Cell 7 (10) (2008) 1733–1741, https://doi.org/10.1128/EC.00253-08.
[33] A. Basseville, P.C. Violet, M. Safari, C. Sourbier, W.M. Linehan, R.W. Robey, M. Levine, D.L. Sackett, S.E. Bates, A histone deacetylase inhibitor induces acetyl-CoA depletion leading to lethal metabolic stress in RAS-pathway activated cells, Cancers (Basel) 14 (11) (2022) 2643, https://doi.org/10.3390/cancers14112643.
[34] C. Murciano, D.L. Moyes, M. Runglall, P. Tobouti, A. Islam, L.L. Hoyer, J.R. Naglik, Evaluation of the role of Candida albicans agglutinin-like sequence (Als) proteins

in human oral epithelial cell interactions, PloS One 7 (3) (2012) e33362 doi: 10.1371/journal.pone.0033362. PMID: 22428031; PMCID: PMC3299778.
[35] A. Mottola, B. Ramírez-Zavala, K. Hünniger, O. Kurzai, J. Morschhäuser, The zinc cluster transcription factor Czf1 regulates cell wall architecture and integrity in Candida albicans, Mol. Microbiol. 116 (2) (2021) 483–497, https://doi.org/10.1111/mmi.14727.
[36] M.L. Langford, J.C. Hargarten, K.D. Patefield, E. Marta, J.R. Blankenship, S. Fanning, K.W. Nickerson, A.L. Atkin, Candida albicans Czf1 and Efg1 coordinate the response to farnesol during quorum sensing, white-opaque thermal dimorphism, and cell death, Eukaryot. Cell 12 (9) (2013) 1281–1292, https://doi.org/10.1128/EC.00311-12.
[37] R. Martin, D. Albrecht-Eckardt, S. Brunke, B. Hube, K. Hünniger, O. Kurzai, A core filamentation response network in Candida albicans is restricted to eight genes, PloS One 8 (3) (2013) e58613, https://doi.org/10.1371/journal.pone.0058613.
[38] G. Huang, H. Wang, S. Chou, X. Nie, J. Chen, H. Liu, Bistable expression of WOR1, a master regulator of white-opaque switching in Candida albicans, Proc. Natl. Acad. Sci. U. S. A. 103 (34) (2006) 12813–12818, https://doi.org/10.1073/pnas.0605270103.
[39] B.L. Granger, Accessibility and contribution to glucan masking of natural and genetically tagged versions of yeast wall protein 1 of Candida albicans, PloS One 13 (1) (2018) e0191194.
[40] I. Tsarfaty, H. Sandovsky-Losica, L. Mittelman, I. Berdicevsky, E. Segal, Cellular actin is affected by interaction with Candida albicans, FEMS Microbiol. Lett. 189 (2) (2000) 225–232, https://doi.org/10.1111/j.1574-6968.2000.tb09235.x.
[41] B. Schindler, E. Segal, Candida albicans metabolite affects the cytoskeleton and phagocytic activity of murine macrophages, Med. Mycol. 46 (3) (2008) 251–258, https://doi.org/10.1080/13693780701837157.
[42] D.D. Mosel, R. Dumitru, J.M. Hornby, A.L. Atkin, K.W. Nickerson, Farnesol concentrations required to block germ tube formation in Candida albicans in the presence and absence of serum, Appl. Environ. Microbiol. 71 (8) (2005) 4938–4940, https://doi.org/10.1128/AEM.71.8.4938-4940.2005.
[43] S. Su, X. Li, X. Yang, Y. Li, X. Chen, S. Sun, S. Jia, Histone acetylation/deacetylation in Candida albicans and their potential as antifungal targets, Future Microbiol. 15 (2020) 1075–1090, https://doi.org/10.2217/fmb-2019-0343.
[44] R.A. Calderone, W.A. Fonzi, Virulence factors of Candida albicans, Trends Microbiol. 9 (7) (2001) 327–335, https://doi.org/10.1016/s0966-842x(01)02094-7.
[45] M. Cicuéndez, L. Casarrubios, M.J. Feito, et al., Candida albicans/macrophage biointerface on human and porcine decellularized adipose matrices, J Fungi (Basel). 7 (5) (2021) 392, https://doi.org/10.3390/jof7050392.
[46] D.H. Navarathna, K.W. Nickerson, G.E. Duhamel, T.R. Jerrels, T.M. Petro, Exogenous farnesol interferes with the normal progression of cytokine expression during candidiasis in a mouse model, Infect. Immun. 75 (2007) 4006–4011, https://doi.org/10.1128/IAI.00397-07.